

# AI-Based Electrode Optimisation for Small Satellite Ion Thrusters

Árpád László Makara<sup>1</sup>, András Reichardt<sup>2</sup> and László Csurgai-Horváth<sup>3</sup>

**Abstract**—Computing capacities for numerical modelling are available to an unprecedented extent today. The spread of various artificial intelligence (AI) -based solutions (which in many cases are also resource-intensive operations) is also facilitated by this increase in capacity, which offers several new opportunities in this area. On the one hand, optimization tasks can be done quickly, on the other hand, it is also possible to solve (estimate) problems where we cannot (for some reason) create a model for the initial problem. In our article, we investigate how to apply artificial intelligence-based solutions to electromagnetic field computing tasks as efficiently as possible. The required theoretical summary presents an implemented application: optimization of electrostatic ion engine accelerator electrodes for orbit correction operations. To solve each problem, we used methods from the supervised machine learning toolkit, usually along with LMS (least mean square method) update steps. All inputs required for AI were solved by numerical space calculation (primarily using the finite element method). The data input required to optimize the electrodes of an ion thruster can come from two sources: measurement data or simulation results. Given that the operating environment of a satellite can be modelled in a vacuum chamber, it is a particularly difficult issue to perform the measurement, but even more difficult in the case of optimisation. Therefore, an effective solution to the problem can only be achieved by simulation. The primary goal of this research is to optimise the fuel (in this case, the number of ions) during operation, with the stated aim of maximising the time of operation of the spacecraft.

**Index Terms**—ion thruster, electrode, optimisation, simulation, artificial intelligence, small satellite

## I. INTRODUCTION

The launch system of a spacecraft is a complex structure and it consists of typically several rocket stages that often use different types of high-power propulsion systems. A typical and commonly applied structure can be observed in the Ariane rocket family [1]. Usually high-power booster(s) with solid propellant can be found in the first stage, extended with a cryogenic core stage with liquid propellant. The boosters are operating in the first launch phase for a couple of minutes and after the separation are returning to the ground for later reuse. The main stage operates up to its separation when the spacecraft's performance value an appropriate height and speed reached. At this point the upper stage is ignited to place the payload(s), e.g. satellite(s) to their final orbit.

<sup>1,2,3</sup> Budapest University of Technology and Economics Department of Broadband Infocommunication and Electromagnetic Theory, Budapest, Hungary

<sup>1</sup> corresponding author (e-mail: makara.arpadlaszlo@edu.bme.hu)

<sup>2</sup> (e-mail: reichardt.andras@vik.bme.hu)

<sup>3</sup> (csurgai-horvath.laszlo@vik.bme.hu)

The above-mentioned rocket engines are providing very high thrust in the kN-MN range for several minutes of duration. When the satellite already reached its planned height and speed the propulsion system supports the spacecraft's further orbital maneuvers and changes its position by firing thrusters. Depending on the mission's type, the task of the propulsion subsystem may perform apogee injection e.g. to reach a final geostationary orbit. For that one a few hundred of N thrust level is required. In order to perform minor orbit control, like modifying the inclination, maintenance of the orbit, low power thrusters with few times 10N is required. The orientation of a satellite should be also controlled in order to maintenance the spin rate, perform axes stabilization or rotate the satellite to a specific direction. This kind of maneuver requires a few N of thrust.

Satellite propulsion subsystems have many different operating principles and may use different propellant types. Chemical propulsion systems with monopropellants or bipropellants may provide higher thrusts. However, the resulted chemical products may influence the external environment of the spacecraft and it could be intolerable by the mission's goal, especially when there are sensitive measurement devices among the payloads. Cold gas systems with neutral gases are operating in the lower power ranges. The primary choice is nitrogen as its relatively large molecular size prevents the fuel leakage. An alternative propellant is argon, when nitrogen cannot be applied for specific reasons.

The electric propulsion systems are using ionizable gases as the propellant. Electrical power supplied by an external energy source is used to accelerate the propellant to extreme velocities and thereby achieve very high specific impulses. However, the power as well as the thrust is limited by the available electrical energy delivered by batteries, solar generators or radioisotope thermoelectric generators (RTGs). The electric propulsion systems have very low thrust, comparing to the previous methods. Thrusters for electric propulsion require propellants which can be easily evaporated and ionized and which have a high molecular weight. Therefore the development of thrusters for electric propulsion concentrated on the use of inert gas xenon, which can be stored in high-pressure gas tanks. Xenon has a high molecular weight and can be quite easily ionised. The idea of electric propulsion is not new - NASA Glenn Research Center has been a leader in ion propulsion technology development since the late 1950s, with its first test in space - the Space Electric Rocket Test 1— flying

on July 20, 1964 [2]. In [3] and [4] the principles of operation and the several types of thrusters that are either operational or in advanced development are discussed. Ion thrusters (based on a NASA design) are now being used to keep over 100 geosynchronous Earth orbit communication satellites in their desired locations and there are other missions with electric propulsion system as well.

To the beginning of 2021, the use of ion thrusters has once again come to the fore [5]. An open question for the future, which is the minor version for an ion thruster that can work (especially for small satellites in space orbits close to Earth). To minimise it, on the one hand, it is necessary to choose the right fuel. On the other hand, adapting the structure of the spacecraft to this. Previous simulation results available in the literature are primarily particle-based plasma simulations, all of which are faithfully modeled by a given arrangement (such as the T5 model, flow simulation of an electrostatic ion thruster [6]).

One possible, well-functioning method for electrostatic ion engines is Monte Carlo Collision Method-based simulations [7]. Another proven method is the PIC (Particle In Cell) to solve the problem, for which we can see results for DPI [8]. Also worth mentioning is the Hall Thrusters, where the magnetic field is also present in the direction of the plasma. Such simulation expiration dates are fundamentally more complex than the electrostatic cases that are the subject of recent research [9].

The most crucial goal of the current research is to investigate the effect that can be achieved by controlling the potential of each individual electrode when using electrostatic ion thrusters. Based on the available results, two assumptions should be take into account in order to get correct results: first of all, ions must not condense on the electrodes or on any component of the spacecraft, including other ions. On the other hand, the density and initial direction of the ions in the space of the accelerator electrodes cannot be arbitrary. With this approach, it is primarily possible to study how the movement of ions can be influenced by changing the potentials, and based on this, the amount of fuel consumption can be optimized. The results of the current research were designed for a general structure, while using typical values from previous spacecraft.

The design of the acceleration electrodes of ion thrusters is a complex problem. In ground conditions only vacuum-chamber measurements are appropriate to simulate the real conditions of space, that is a particularly complex issue. Therefore simulations are feasible solutions in order to develop and optimize the electrodes. The problem area is an electromagnetic field computing task where applying an AI-based method is a novel and encouraging approach to develop the optimal accelerator electrodes of ion thrusters. In this paper we provide a finite element based solution to calculate quasi-electrostatic field of the internal of the thruster and we perform simulations on the outlets. The applicability of this thruster method for small satellites is also investigated.

The organization of this paper is as follows. Section II. provides a brief introduction to electric engines. Section III. describes the presentation of our ion engine model made in the earlier phase of the research [10]. In Section IV., we

present the ion engine optimisation implemented based on our simulation model. Last but not least, in Section V. we summarise our results.

## II. PRINCIPLES OF ION ENGINE OPERATION

### A. Electric propulsion engine types

Electric propulsion (EP) can be categorized by different ways [11]. First type of ion thrusters are utilizing only electric field to accelerate ions (see Fig. 1.). The other type is using magnetic field and electric field to accelerate and control ion or plasma jets [4]. This type is more sophisticated but due to its size, it is not possible to implement within CubeSat dimensions (the standard dimension 1 unit CubeSat is 10 cm × 10 cm × 10 cm size) [12]. Both types are using electric field acceleration grid (AG). It is formed as two grids separated from each at a few centimeters having a potential difference between them. Ions are entering through the input grid and leaving through the output grid at a higher speed.

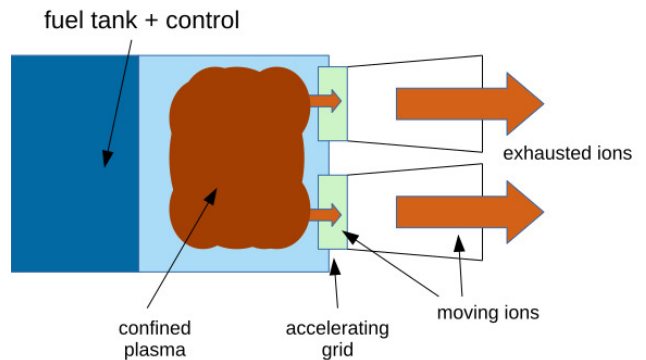


Fig. 1. Principle of an ion thrust engine operation.

### B. Electric propulsion system proposed

We propose a simple electric propulsion system for small satellites based on the principle by accelerating an ionized gas moving outward of the spacecraft and thrusting the spacecraft to the opposite direction. The gas should be charged (ionised) allowing the acceleration by electric field. Our model is based on a simple discharge chamber where gas is ionized and an acceleration grid that moves ions outward. Control of ion jets are performed using electrodes attached to the inner surface of the nozzle and driven by a potential. In this paper we analyze the ion jet control inside the nozzle by applying only an electric field.

### C. Possible system for CubeSats

CubeSats have limited space and mass. Currently there are spinoffs offering a 2 unit large propulsion system based on xenon or iodine [13]. With this system, an additional steering mechanism can be used to change the orientation of the satellite based on deflecting ions flying out from the thruster. The deflector system can bend the beams, and thereby it can help to maneuver the satellite. The system is shown on Fig. 2.

The rectangular formations are the electrodes of the deflector system. It can turn the ion beam and thereby it can turn the satellite too.

The arrangement shown in Fig. 1. is used in the present research. We did not examine how the plasma will be produced, handled, stored and how to control the flow of sufficient ions into the accelerator space. Furthermore, the modeling of the hollow electrode is also neglected.

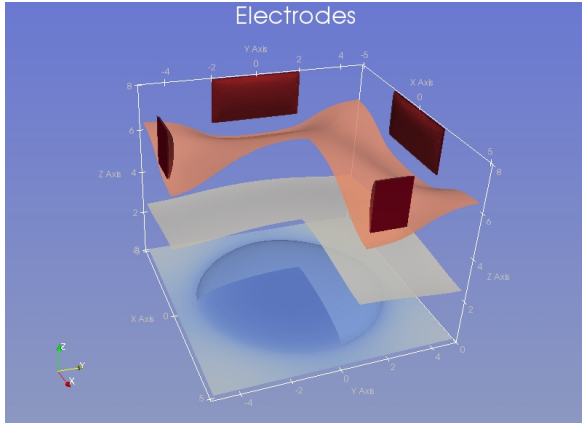


Fig. 2. Outline of the nozzle. Small rectangles on the sides are control electrodes. The tube on the bottom is the upper side (top side) of the acceleration grid. The top of the grid is connected to zero voltage. The potential of the electrodes is used to control ions movements. Sizes are measured in centimeters. Only for the first row of electrodes shown.

### III. SIMULATION OF AN ELECTROSTATIC THRUSTER

The electromagnetic field created by control electrodes can be modeled as a constant field with very slow change in time [14]. We disregard the physical extent of the ions, only their mass counts for acceleration. The ions have a sufficiently low density in the space between the accelerator electrodes to correct the assumption that they do not collide with each other and that the field they create is negligible. Then the electrostatic Laplace-Poisson equation is as follows (the partial differential equation, PDE):

$$\nabla \varepsilon_0 \nabla \varphi = 0. \quad (1)$$

where  $\varepsilon_0$  is the vacuum permittivity,  $\varphi$  is the potential. In the simulation region we solve equation (1) with boundary conditions (see Section III-A.) and get the field that moves the ions. The problem was solved by the finite element method (FEM). A possible arrangement of the nozzle is shown in Fig. 3. The force acting on the embankments can be expressed by Lorentz's law [15]:

$$\mathbf{F} = q(\mathbf{E} + \mathbf{v} \times \mathbf{B}) \quad (2)$$

where  $\mathbf{F}$  is the force,  $q$  is the charge of the moving particle,  $\mathbf{E}$  is the electric field,  $\mathbf{v}$  is the velocity of the moving particle and  $\mathbf{B}$  is the magnetic induction. The field  $\mathbf{B}$  generated by the hum of the ions is negligible compared to the effects of the

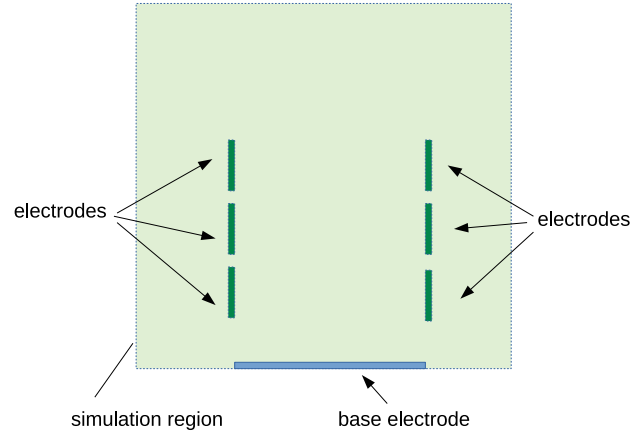


Fig. 3. Geometry of simulated rectangular shaped nozzle

electrodes, and the change in the potentials of the electrodes is slow enough hence their effects are not significant.

After solving this model we can calculate the trajectory of ions starting from base electrode by solving equation of motion (3) (which is the Newton's second law) with force calculated from potential (4), [16]:

$$m_{\text{ion}} \cdot \frac{d^2 \mathbf{r}}{dt^2} = \mathbf{F} \quad (3)$$

$$\mathbf{F} = (-1) \cdot q_{\text{ion}} \cdot \nabla \varphi \quad (4)$$

where  $\mathbf{r}$  is the local vector of the moving ion,  $t$  is the time.

The current research is limited to two-dimensional cases for faster runtime. A simulation result (the red line is the route of a single moving ion) is shown in Fig. 4., which was generated using MATLAB PDETool [17]. The three-dimensional case is a magnitude difference in computing capacities. While in the two-dimensional case the steps are of the order of  $\mathcal{O}(N^2)$ , in this case  $\mathcal{O}(N^3)$ , where  $N$  is the number of FEM simulations elements (degrees of freedom). The more accurate the simulation result we intend to achieve, the more points we need (denser mesh). For our method, this is the most resource-intensive part where we chose the smaller one.

The effect of the actual ion beam is negligible from the point of view of simulation so that the constituent ions can be simulated one by one. Then it is enough to calculate the resulting  $\mathbf{E}$  field and then the motion of each ion. The force of the thruster radius can be calculated as a result of these individual forces. This approximation is valid as long as the resulting electric field strength is given by the potential of the electrodes.

#### A. The boundary conditions

There are two ways to consider different physical objects during FEM simulation. One possible solution is to represent it in material parameters (application of non-zero charge density or relative dielectric constant in sub-areas). The other is to apply boundary conditions (BC) [18].

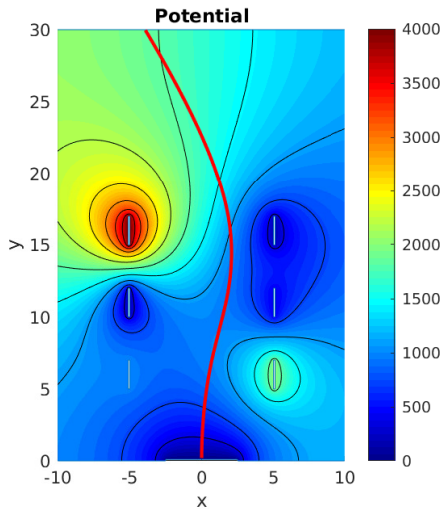


Fig. 4. Electrostatic potential simulated (colored contour) and particle trajectory (red line). Sizes are measured in centimeters.

Each electrode in the simulation means a Dirichlet-type boundary condition. There are two practical reasons for this: from an operational point of view, only the effect of potential is interesting, and on the other hand, its value can be easily optimised. Denote the potential of the  $i^{\text{th}}$  electrode by

$$\varphi_i = U_i \quad (5)$$

It is necessary to select a reference point with a value of zero, for which the base electrode is best suited (see Fig. 3.). This is not a real electrode but a connecting hole between the plasma space and the acceleration space. In the two-dimensional model, this is also a similar boundary condition to the real electrodes, with only a constant zero voltage.

It is necessary to handle the space environment at a sufficient distance from the substantial part of the ion thruster (see Fig. 3.). In a typical operating environment of the small satellites, charged particles are present in negligible amounts. Therefore, the atmosphere acts as a kind of ideal insulator that can be modelled with a homogeneous Neumann-type boundary condition:

$$\frac{\partial \varphi}{\partial n} = 0 \quad (6)$$

That is enough for the simulation. To describe more accurately a real-world system, it would still be necessary to model the environment of the satellite and the electrodes (such as frame, electronics, etc.). With both boundary conditions and material properties, these can be perfectly modelled; however, they are not required for current research results, so we omit them for the sake of simplicity.

#### IV. OPTIMISATION

Optimisation of parameters means, on the one hand, the physical parameters of the spacecraft and, on the other hand, the optimisation of operational resources. For each satellite,

the following parameters can be modified to optimise the expected performance:

- the geometry of the electrodes and the thruster,
- the type of ion used as fuel,
- number of accelerator electrodes,
- size of the accelerator electrodes
- electrode potential.

In the case of small satellite design, the standards and mission goal essentially limit the possibilities of the spacecraft size and weight, so there is no possibility for large-scale optimisation here. Therefore, the primary goal is to optimise the use of energy (typically electricity) and fuel (in this case, the number of ions) during operation, with the stated aim of maximising the time of operation of the spacecraft. In the case of electrostatic ion engines, the desired thrust can be achieved along with two strategies: accelerating more ions with lower voltages or accelerating less fuel particles with much higher energies than before. A longer operating time can be ensured for the thruster unit if the ions are available for as long as possible. This cannot be easily replaced, so the task is to minimise the fuel (ion) consumption.

Thus, the subject of the current research is the optimisation of the individual operational parameters.

##### A. Parameter optimization

As we know the expected movement of our spacecraft, so the application of supervised machine learning is necessary. Given that the partial differential equation of the electrostatic model presented in the simulation part describes the desired behaviour with sufficient potential, the regression problem itself is given.

The surface of each electrode can be considered equipotential. The values of this form is the weight vector  $\mathbf{W}$  (where  $\mathbf{W} = [U_1, U_2, \dots, U_N]^T$ ,  $i$  is the  $i^{\text{th}}$  electrode potential). These values are, by the way, the boundary conditions of the FEM model presented in Section III. The error function is interpreted as follows:

$$K = e^2(k) = [t(k) - a(k)]^2 \quad (7)$$

where  $e$  is the value of the error,  $t$  is the expected output,  $a$  is the instantaneous value of the estimate, and  $k$  is the number of iterations. The error is actually the difference between the expected trajectory of each ion and the simulation result. This difference can be defined according to several approaches, which will be discussed in more detail in Section IV-B. The task is to minimize the resulting  $K$  error function, thus optimizing the orientation corrections. This optimisation is implemented with supervised machine learning within that the Least Mean Square method [19]:

$$\mathbf{W}_{\text{next}} = \mathbf{W}_{\text{prev}} + 2 \cdot \mu \cdot e \cdot \mathbf{p} \quad (8)$$

where  $\mu$  is the learning-rate,  $e$  is the error,  $\mathbf{p}$  is scaling factor or input parameters. Using an LMS iterative procedure, the residuum part will always remain, which can be somewhat reduced by averaging the repeated calculations. The optimisation flowchart is shown in Fig. 5.

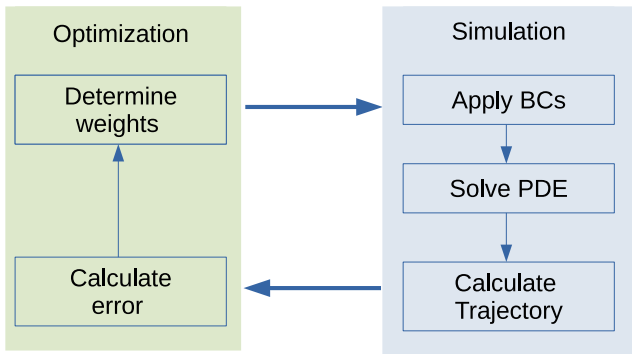


Fig. 5. Schematic flow chart of the optimization and simulation process as an infinite loop.

### B. Choosing the target

One of the most important pillars of the supervised machine learning is the designation of target states ( $t$ ). If this is flawed (or distorted), the training process will not move towards the ideal solution. In the present case, taking advantage of the momentum retention, we expect that the ion beam is pushing the spacecraft along this path. In doing so, the trajectory of each ion must be determined. This can be done either by prescribing control points or control regions. Fig. 6. shows a 4-zone control arrangement.

The error is actually the distance between the control point or zone and the ion trajectories at a given altitude:

$$e_i = t_i - a_i = \text{distance}(a_x, c_x)|_{y=\text{const}} \quad (9)$$

where  $e_i$  is the  $i^{\text{th}}$  control zone error,  $a_x$  is the ion place, in a given altitude, and  $c_x$  is the control zone at same altitude. In the case of parameters with acceleration and velocity dimensions, it is expedient to prescribe the control zone in the width of the entire calculation range or to interpret the control moment on a time basis. Distance means Euclidean distance for each quantity.

When prescribing a route, it is worth defining these points at several heights, and by applying a weighting form the resulting error is:

$$e = \frac{1}{N} \sum_{i=1}^N \omega_i (t_i - a_i) \quad (10)$$

where  $w$  is the given control point's scaling/importance factor,  $N$  is the number of the control points/zones.

The role of each control point is different. At the beginning of the arrangement (close to the base electrode), their primary function is to prevent ions from collision with the electrodes. In contrast, the points at the end of the engine are almost exclusively responsible for orienting the ion in the correct direction. It is advisable to use as many control elements that are still proportional to the degrees of freedom (this is actually a nonlinear curve fitting task). The width of the zones should be selected in proportion to the width of the starting point and the initial angle of the ions. If we select too many reference points, two things can happen. First, the number of iterations required can be greatly increased. On the other hand,

it is conceivable that the error function will have several local minimal relatively close to each other, and the algorithm will jump between each other. The latter is especially typical for small-angle turns, where straight travel also results in a small error. In Fig. 7. there is a relatively small degree case with well-chosen control points.

### C. More complex error criteria - status based error

Not only the path of the ion but also its other parameters may be useful. Typically, this can be the value of acceleration (per coordinate) and its position (also per coordinate). There is a set of adjustable parameters (i.e., voltage of the accelerator electrodes) on which all the parameters we are looking for depending. For each element of the state, we can write an error function as before. There is no certainty that the zero position of each function will be in the same place. For this reason, we need to prioritize which parameter is how important to us. Of course, we can also define criteria that are interpreted not at a specific place but at a given time (after a step). Then the name of the reference value is correct, but the procedure is the same.

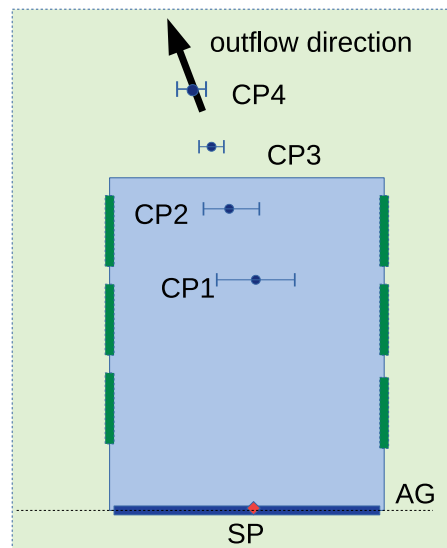


Fig. 6. Control points of trajectory definition. CPs are control points, where ions should fly through. AG is the top of acceleration-grid, SP designates starting point.

As it was shown in the previous subsection the cost function with highest priority is optimised. The potentials are then adjusted according to the next parameter in the sequence, taking care that the higher priority parameter cannot deteriorate by more than a predefined value. As soon as the error has been reduced to a sufficient level, the next parameter is consumed, taking care that two values cannot deteriorate more than the individual limit.

In fact, we do the same thing as in the case of tension. We narrow down the range of possible solutions, thus most likely ignoring the best solution. Calculating the parameters at a lower location in the priority queue is actually a "roaming" around the optimum of another parameter, looking for a good

location suitable for both values. The steps in the procedure are the following:

- 1) Optimisation of the parameter with highest priority (typically by averaging multiple runs),
- 2) Specify fault tolerance,
- 3) Optimisation of the second parameter in the priority queue (similar to the first point) so that the error for the higher priority parameters cannot leave the tolerance band,
- 4) Repeating steps 1.-3. so that the tolerance values for the higher priorities cannot be violated by each optimisation.

#### D. Choosing the input parameters or the scaling factor

The parameter  $\mathbf{p}$  can be denoted with two names: an input parameter or a scaling factor. The former is a common name for typical neural networks, which can be used in the present case. The latter presupposes a higher level of abstraction, where each parameter loses its physical meaning and encodes a prior knowledge [20]. Regardless of interpretation, the values of  $\mathbf{p}$  affect the learning rate ( $\mu$ ):

$$\mathbf{P} = \mathbf{p} \cdot \mathbf{p}^T. \quad (11)$$

The maximum eigenvalue ( $\lambda_{max}$ ) or trace of the  $\mathbf{P}$  matrix is critical. The reciprocal of this value is an upper limit on the maximum value of the learning rate to keep the process stable [20]:

$$\mu_{max} < \frac{1}{\lambda_{max}} \leq \frac{1}{\text{trace}\mathbf{P}}. \quad (12)$$

In the case of assigning a physical input parameter to the same voltages, the natural choice is the surface (or, in two-dimensional cases, the perimeter) of each electrode. This is actually the same as the boundary condition area within our FEM model calculation range. This actually means that each potential is weighted by the size of the electrodes. The process can be speeded up by consistently multiplying the values one of the sides by minus one. Thus, the opposing electrodes receive a more drastic change during each update step. Overall, the system converging faster towards the solution; however, the voltage values of each electrode pair may oscillate at the beginning of the process.

In the present arrangement, the process can be accelerated (slowed down if incorrectly selected) if the vector  $\mathbf{p}$  is a scaling factor (or more complex, a scaling function). In this case, the prior knowledge should be used that towards the end of the arrangement, the current electrodes contribute more to the translation than the previous ones. Thus, in the present study, the values of these scale factors were typically chosen to be larger than the others (usually by an order of magnitude). During testing, in most (but not always) cases, we found that the residual error value ( $K$ ) was closer to zero than if we had chosen them equally. No drastic acceleration was generally observed in the number of iteration steps (except for a few more specific cases). However, due to the more precise fit, the expected result can be found sooner, so overall it is faster to find the potentials for each form of movement. Presumably, one possible improvement of the procedure would be to create a deterministic, more efficient scaling rule.

Variation of the input parameter/scaling factor can be understood as a time-varying iteration rate. In the event that we do so and start from a large value in time (so that the process is still stable), we take advantage of the rapid initial changes in the LMS. After a few iterations (typically 20-30), it is advisable to reduce its value cyclically. This reduces the rate of change but also the value of the residuum part. In the tests performed in the current research, we found that with well-chosen scaling factors, the procedure usually takes the order of 100 steps. Thus, in essence, the calculation of a given form of movement (the most resource-intensive element of which is the FEM simulation) can be solved even on a personal computer.

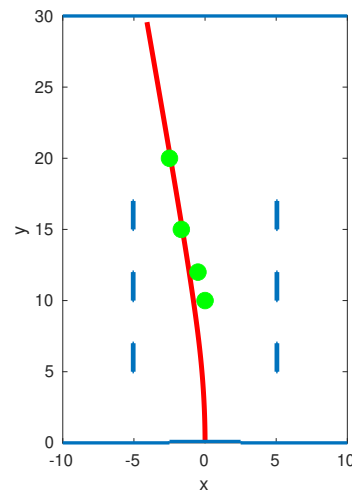


Fig. 7. Optimization result with control points. Sizes are measured in centimeters.

#### E. Physical limitations

There are several physical constraints that need to be respected to optimise the space of the model. For a non-relativistic initial model, the first and most important is to figure out the velocity of ions. In the case where the velocity of each ion becomes comparable to the speed of light (e.g., it reaches 10% of the speed of light), the result becomes increasingly inaccurate. The procedure would give a false result also if the speed of light was not the maximum of the available speed. However, it is necessary for the algorithm to indicate when the ions are achieved at this speed.

Another critical physical limitation is the finite voltage of the electrodes. In the case of a spacecraft, of course, the voltage level can only be produced in a specific range. This can typically be on the order of a few kV [8]. This can be different for every electrodes. The output of the optimisation step must always satisfy the following inequality:

$$\mathbf{U}_{min} \leq \mathbf{W} \leq \mathbf{U}_{max} \quad (13)$$

where  $U_{min}$  is the lower and  $U_{max}$  is the upper limit for the possible voltage value in the spacecraft. It can be interpreted as both continuous and discrete quantities.

By not allowing the electrodes to take on any value, some of the minimum possible locations of the function  $K$  are omitted. A trivial example of this is when we prescribe as

much acceleration as possible (without an upper bound). An obvious solution is to shape the most significant accelerating potentials, but the physical limitations of the spacecraft do not allow it. Thus, the task is to find the best solution in a local environment of the error function.

V. CONCLUSION

We presented the first results of a system that can control ion thruster’s ion beam using only electric field. The effect of guiding electrodes can be controlled by the magnitude of electrode potential and connection status of the other electrodes. It is found that thrusting material does not affect the ability to control. A solution based on the optimisation of boundary conditions provides a result within an acceptable number of iteration steps. The process is fast and easy to parameterise. In addition, the procedure can be independent of the model and can be applied to a more complex physical thruster. The topic of future research is how to interpret the error in the case of three-dimensional procedures. In this paper, we examined only one starting point and start velocity; it is straightforward to use more points and velocities to optimise. Of course, such a simple optimisation can not be used to completely resolve that problem. In our future work, we intend to examine the usability of the more complex error function and three-dimensional arrangements.

REFERENCES

[1] Arianespace, *Ariane 5 User’s Manual Issue 5 Revision 2*. Ariane, Oct. 2016.

[2] Ronald J. Cybulski, Daniel M. Shellhammer, Robert R. LoveII, Edward J. Domino, and Joseph T. Kotnik, *RESULTS FROM SERT I ION ROCKET FLIGHT TEST*, 1965th ed.

[3] J. E. Pollard, D. E. Jackson, D. C. Marvin, A. B. Jenkin, and S. W. Janson, “Electric propulsion flight experience and technology readiness,” Jun. 1993. [Online]. Available: <https://arc.aiaa.org/doi/abs/10.2514/6.1993-2221>

[4] K. Holste, P. Dietz, S. Scharmann, K. Keil, T. Henning, D. Zschätzsch, M. Reitemeyer, B. Nauschütt, F. Kiefer, F. Kunze, J. Zorn, C. Heiliger, N. Joshi, U. Probst, R. Thüringer, C. Volkmar, D. Packan, S. Peterschmitt, K. T. Brinkmann, H.-G. Zaunick, M. H. Thoma, M. Kretschmer, H. J. Leiter, S. Schippers, K. Hannemann, and P. J. Klar, “Ion thrusters for electric propulsion: Scientific issues developing a niche technology into a game changer,” *Review of Scientific Instruments*, vol. 91, no. 6, p. 061101, Jun. 2020. [Online]. Available: DOI: 10.1063/5.0010134

[5] I. Levchenko, S. Xu, G. Teel, D. Mariotti, M. L. R. Walker, and M. Keidar, “Recent progress and perspectives of space electric propulsion systems based on smart nanomaterials,” *Nature Communications*, vol. 9, no. 1, p. 879, Dec. 2018. [Online]. Available: <http://www.nature.com/articles/s41467-017-02269-7>

[6] M.JugrootandJ.K.Harvey, “Simulation of flows within an electrostatic ion thruster for space missions,” *The Aeronautical Journal* (1968), vol. 105, no. 1053, p. 613–618, 2001.

[7] B.Korkut,Z.Li,andD.A.Levin, “3-d simulation of ion thruster plumes using otree adaptive mesh refinement,” *IEEE Transactions on Plasma Science*, vol. 43, no. 5, pp. 1706–1721, 2015.

[8] J. Wang, D. Brinza, and M. Young, “Three-Dimensional Particle Simulations of Ion Propulsion Plasma Environment for Deep Space I,” *Journal of Spacecraft and Rockets*, vol. 38, no. 3, pp. 433–440, May 2001. [Online]. Available: <https://arc.aiaa.org/doi/10.2514/2.3702>

[9] K. Shan, Y. Chu, Q. Li, L. Zheng, and Y. Cao, “Numerical Simulation of Interaction between Hall Thruster CEX Ions and SMART-1 Spacecraft,” Jun. 2015. [Online]. Available: [https://www.researchgate.net/publication/282494427\\_Numerical\\_Simulation\\_of\\_Interaction\\_between\\_Hall\\_Thruster\\_CEX\\_Ions\\_and\\_SMART-1\\_Spacecraft](https://www.researchgate.net/publication/282494427_Numerical_Simulation_of_Interaction_between_Hall_Thruster_CEX_Ions_and_SMART-1_Spacecraft) DOI: 10.1155/2015/418493

[10] A. Makara, A. Reichardt, and L. Csurgai-Horváth, “Visualization and simulation of ion thrusters possibly usable by small satellites, In Selected papers of 6th International Conference on Research, Technology and Education of Space (H-SPACE 2020).” HSPACE2020-FP-59, 2020: Hungarian Astronautical Society, Feb. 2020. [Online]. Available: [http://space.bme.hu/wp-content/uploads/2021/01/Proceedings\\_Papers\\_HSPACE-2020.pdf#page=62&zoom=74,0,9](http://space.bme.hu/wp-content/uploads/2021/01/Proceedings_Papers_HSPACE-2020.pdf#page=62&zoom=74,0,9)

[11] D. Krejci and P. Lozano, “Space propulsion technology for small spacecraft,” *Proceedings of the IEEE*, vol. 106, no. 3, pp. 362–378, 2018.

[12] E. Kulu, ‘What is a CubeSat?’, Nanosats Database. [Online]. Available: <https://www.nanosats.eu/cubesat> [Accessed: Dec. 18, 2021]

[13] ThrustMe, “ThrustMe,” 2021, <https://www.thrustme.fr/>. [Online]. Available: <https://www.thrustme.fr/>

[14] R. G. Jahn and E. Y. Choueiri, “Electric Propulsion,” in *Encyclopedia of Physical Science and Technology*. Elsevier, 2003, pp. 125–141. [Online]. Available: <https://linkinghub.elsevier.com/retrieve/pii/B0122274105002015> DOI: 10.1016/B0-12-227410-5/00201-5

[15] M. CHEN, A. SUN, C. CHEN, and G. XIA, “Particle simulation of grid system for krypton ion thrusters,” *Chinese Journal of Aeronautics*, vol. 31, no. 4, pp. 719–726, 2018. [Online]. Available: <https://www.sciencedirect.com/science/article/pii/S1000936118300384> DOI: 10.1016/j.cja.2018.01.020

[16] R. W. Hockney and J. W. Eastwood, *Computer Simulation Using Particles*, 1st ed. Bristol England; Philadelphia: CRC Press, Jan. 1989.

[17] MATLAB, “Partial Differential Equation Toolbox,” 2021. [Online]. Available: <https://www.mathworks.com/products/pde.html>

[18] K. Simonyi, *Theoretische Elektrotechnik*. Leipzig: Barth, 1993.

[19] K. P. Murphy, *Machine learning: a probabilistic perspective*. Cambridge, Mass. [u.a.]: MIT Press, 2013.

[20] M. T. Hagan, H. B. Demuth, M. H. Beale, and O. D. Jesús, *Neural Network Design*, 2nd ed. Wrocław: Martin Hagan, Sep. 2014.



**Árpád László Makara** is currently a PhD student at the Department of Broadband Infocommunications and Electromagnetic Theory of the Budapest University of Technology and Economics (BME). The topic of his master thesis work was the simulation and optimization of electrostatic ion thrusters for CubeSats. For two semesters, he held exercises at BME for BSc electrical engineering students on the subject of Introduction to Electromagnetic Fields. His current research topic is relating to millimeter wavelength indoor propagation for 5G, and his first results in this field were presented on the EFOP-3.6.2 workshop in November, 2020.



**András Reichardt** is currently a assistant lecturer at Budapest University of Technology and Economics (BME), Department of Broadband Infocommunications and Electromagnetic Theory. His current research interests focus on electromagnetic field calculation, mathematical modeling of complex systems, and equivalent circuit representations of the problems. He currently teaches in many areas such as nanoscience, electromagnetic theory, circuit theory, and discrete signal analysis.



**László Csurgai-Horváth** is employed as an associate professor at Budapest University of Technology and Economics (BME), Department of Broadband Infocommunications and Electromagnetic Theory. His current research interests are focused on indoor and outdoor propagation, measurements and modelling of the rain attenuation on terrestrial and satellite radio links, time series synthesis and cognitive spectrum management. He has been involved in several international projects such as SatNEx, COST Action IC-0802 and QoS MOS. Recently, he has led some ESA-founded research projects relating to the Alphasat propagation and communications experiment and an ESA technology transfer demonstrator project for 5G indoor propagation measurements. Currently, he teaches space technology and channel modelling at BME in Budapest, Hungary.